Astron. Astrophys. 341, 224–232 (1999)

ASTRONOMY
AND
ASTROPHYSICS

Infrared spectroscopy of five short-period Miras and the peculiar Mira Z Ophiuchi

Thomas Lebzelter[1]**, Kenneth H. Hinkle**[2]**, and Josef Hron**[1]

[1] Institute for Astronomy, Türkenschanzstrasse 17, A-1180 Vienna, Austria
[2] Kitt Peak National Observatory, National Optical Astronomy Observatory* 950 N.Cherry Avenue, P.O. Box 26732, Tucson, AZ 85726, USA

Received 8 July 1998 / Accepted 7 October 1998

Abstract. Time-series 2.0–2.5 μm infrared spectra have been observed for Miras with periods less than 200 days. Some of these stars are high velocity and metal poor. We have also observed the peculiar, possibly metal-poor Mira, Z Oph. Velocities, excitation temperatures, and ^{12}C/^{13}C have been determined for these stars. These results are compared with similar data for bright, field Miras. We find Z Oph to be a metal-poor Mira of very low mass-loss rate. All Miras regardless of period, metallicity, or chemical abundance have the same pulsation velocity amplitude. The mode of pulsation is discussed.

Key words: stars: individual: Z Oph – stars: oscillations – stars: AGB and post-AGB – infrared: stars

1. Introduction

More than 50 years ago Wilson and Merrill (1942) pointed out that the kinematic properties of short-period Miras (periods less than 300 days) differ from those of typical field Miras (periods of 300-400 days). The group of Miras of P<300 days is remarkable in having a large scale height perpendicular to the galactic plane and a large velocity dispersion and asymmetric drift relative to the galactic solar motion (Feast 1963, Hron 1991, Alvarez et al. 1997). All these quantities are larger than for Mira variables with longer periods indicating the presence of metal poor objects among this group. This is supported by several spectral characteristics of these stars. Most of these short-period Miras have a selective line weakening in the stronger neutral lines of Fe, Cr, etc.(Merrill 1952). This strongly influences the luminosity classification from classical criteria. As shown by Keenan et al. (1974), high velocity Miras also show a much weaker Ca I line at 4226 Å than Miras with space motions below 85 km s^{-1} and standard stars of luminosity class III. In addition ^{99}Tc is typically not detected in these stars (Little et al. 1987). Lines of Tc are indicators of thermal pulses. The absence of Tc could be due either to low metallicity or to long interpulse times and a decay of Tc before the dredge up. Alvarez et al. (1997), using radial velocities, HIPPARCOS proper motions and ground based photometry, derive parallel period-luminosity relations in the near IR for short and long-period Miras. The short-period Miras turn out to be systematically more luminous. From this difference they estimate a metallicity of the short period Miras of $Z_\odot/16$ which is in agreement with the earlier results of Hron (1991) from photometric colour indices. Such a metallicity is also consistent with the fact that Miras observed in globular clusters all have periods below 300 days (Menzies & Whitelock 1985) and that these clusters belong to the thick disk.

Most likely, the short-period Miras are a mixture of thin disk and thick disk stars with metallicities ranging from solar to about $Z_\odot/16$ (Hron 1993, Jura & Kleinmann 1992). Wyatt & Cahn (1983) found a good correlation between period and age for Mira variables with the oldest objects having the shortest periods. Their kinematic survey indicated main sequence masses for these objects of about one solar mass. Jura (1994) suggests that the progenitors of these short-period Miras might be G stars and he calculates a life time for the Mira phase of 5.10^5 years. A pure sample of thick disk Miras can be found in globular clusters. For these Miras a lower limit for the mass is about 0.8 solar masses.

The low fraction of stars with IRAS data and known radio emission indicates that the average dust and gas mass-loss rate of these stars seems to be lower than for Miras with longer periods. However, the few stars for which mass-loss rates can be determined are probably disk stars and quite comparable to Miras with longer periods (Little-Marenin & Little 1990).

Contrary to the stars with longer periods, all the Miras with periods between 100 and 200 days show very symmetric visual light curves (Vardya 1988). This could be caused by a different pulsational behavior.

Robertson & Feast (1981) found short period Miras to have a different pulsation constant than long period Miras suggesting that they would pulsate in the fundamental mode while the long-period Miras pulsate in first overtone. As discussed by Willson et al. (1982), measurement of the kinematics of stellar photosphere is one approach to testing this suggestion. For the short-period Miras there existed in the literature only kinematic and infrared photometric investigations. Variations in the

Send offprint requests to: LEBZELTER@astro.ast.univie.ac.at

* Operated by the Association of Universities for Research in Astronomy, Inc. under cooperative agreement with the National Science Foundation

infrared spectrum of these stars, which would show pulsational properties much clearer than the optical variations can, have not yet been investigated.

Perhaps the most critical quantity that can be extracted from velocity measurements and used in evaluating the pulsation mode is the amplitude of the radial velocity variations. As shown in previous papers by Hinkle et al. (1982 (HHR), 1984 (HSH) and 1997 (HLS)) Miras with periods between 300 and 400 days show radial velocity amplitudes of about 25 km s^{-1}, while semiregular variables (SRVs), which have periods comparable to most of the short-period Miras discussed here show significantly smaller amplitudes (HLS).

This paper reports on infrared spectroscopy of a small sample of short period Miras. The velocities are measured using CO (Δv = 2) and atomic Ti lines found in the 2.1–2.4 μm region. Hinkle (1978) and Hinkle et al. (HHR, HSH, HLS) report similar measurements for Miras with longer periods. These data for objects with higher metallicity allow a direct comparison of the two groups of variables.

2. Observation and data reduction

The list of program stars consisted of six Miras with periods ranging from 145 through 350 days, RT Cyg, R Vir, SS Oph, Z Oph, R Cet and X Mon. Of these six, RT Cyg, R Vir, SS Oph, and Z Oph, have time series consisting of 3 or more observations. The fundamental properties of these stars as found in the literature are listed in Table 1. A brief summary on other published properties and data of these objects will be given below.

K band (2.1–2.4 μm) spectra were observed with a Fourier Transform Spectrometer at the Kitt Peak National Observatory Mayall 4m telescope. A detailed description of the spectrograph can be found in Hall et al. (1979). The data were taken by KHH between 1985 and 1987. Archival data from 1981 and 1982 taken with the same instrument were also included to improve the phase coverage. The spectra were apodized during the reduction process using the Norton & Beer (1976) function I2. For most of the spectra we achieved a resolution of about 60000 or better. The S/N ratio for the spectra ranges from 15 to more than 100.

The program stars are not as bright as the longer period Miras and SRVs observed by HHR, HSH or HLS. To improve the signal-to-noise ratio the bandpass was limited to the K band. The velocities were measured from the line cores of high and low excitation CO (Δv=2) and stronger titanium lines. The technique used is described in Barnbaum & Hinkle (1995). The velocity of the low excitation CO lines is the mean of 15 lines or more from 2-0 R13 through R41. The velocity of the high excitation CO lines, 2-0 R59 through R87, was calculated from at least 4 lines. About 6 lines were used for each titanium data point. These measurements of single lines were extended by cross correlating all available spectra of our sample in the 4485 to 4535 cm^{-1} region. This region was chosen because there are not too many telluric lines in it. Unfortunately, the program stars have rather weak lines so the cross correlation peak was frequently not strong. These measurements were corrected to heliocentric velocities and were also corrected for small wavelength shifts of the spectrograph by measuring the telluric lines and correcting to this zero point.

Table 1. Properties of the objects observed. Period and spectral type were taken from the General Catalogue of Variable Stars (Kholopov et al. 1985–88, GCVS), radial velocities are from Wilson (1963), except for Z Oph and RT Cyg (Willson et al. 1982). All radial velocities are heliocentric.

GCVS name	IRAS name	period [d]	spectral type	velocity [km s^{-1}]
Z Oph	17170+0133	349.1	K3–M7.5	−86
RT Cyg	19422+4839	190.2	M2–M8.8	−118
SS Oph	16552-0241	180.0	M5e	−33
R Cet	02234-0024	166.2	M4–M9	+42
X Mon	06548-0859	155.8	M1–M6	+162
R Vir	12359+0715	145.5	M3.5–M8.5	−26

The frequency scale in FTS spectra is internally calibrated by the reference laser. Deviation from parallelism between the reference laser and stellar light paths results in the need for a small correction to the frequency scale. The correction is a fixed percentage of the frequency so it can be expressed as a velocity. For the 4 meter FTS the correction is always less than 1 km s^{-1} and is determined by measuring the velocities of about 30 isolated, unsaturated telluric lines in the spectrum. The uncertainty in this correction depends on the S/N of the spectrum but is typically about 0.2 km s^{-1}. The uncertainty of the stellar velocities results from line blending as well as noise in these crowded spectra. The rms uncertainty on a single stellar line is typically 1 or 2 km s^{-1}, so the total uncertainty of the resulting stellar velocities from a set of lines is $0.5 - 1$ km s^{-1}. Due to the small number of unblended high excitation lines the resulting uncertainty on this group of lines is somewhat larger, typically $\sim$1.5 km s^{-1} to 2 km s^{-1}.

3. Sample

The selection of the objects in our sample was mainly driven by limitations of the 4 m FTS. The program stars (with the exception of Z Oph at K=+4.2) are the northern (declination $>$ -10) Miras with K band magnitudes of +3 or brighter and periods less than 200 days. The magnitude limit was imposed by the technology and made it possible to obtain high resolution spectra of moderate signal-to-noise ratio in a few hours of integration. Nevertheless, the short-period Miras of our sample are representative for the short-period Miras. This is illustrated in Fig. 1 which shows the LSR radial velocities versus $V_{max} - K$ for a larger sample of Miras with periods below 200 days taken from Hron (1991, 1998). As described by Hron (1991), $V_{max} - K$ is a temperature indicator which can also be used to roughly discriminate between thin and thick disk (metal poor) Miras. The likely colour boundary is indicated in the figure. The velocities and colours of RT Cyg, X Mon and R Vir indicate that these are metal poor objects while R Cet and SS Oph belong to the thin disk. Alvarez et al. (1997) classify only RT Cyg and X Mon as

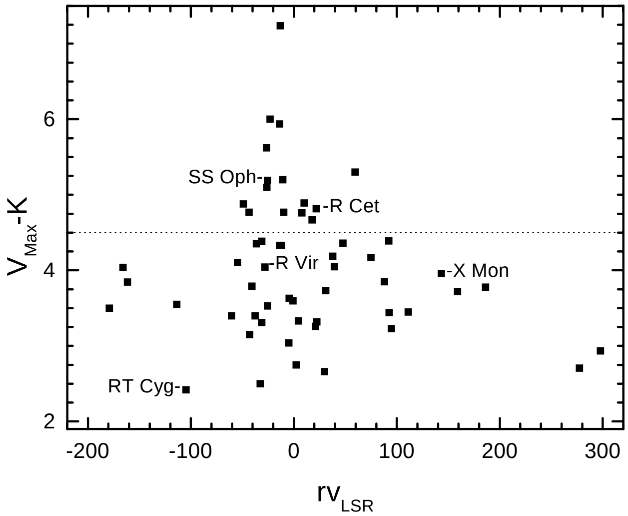

Fig. 1. LSR radial velocity versus $V_{max} - K$ for a sample of short-period Miras. The objects used in our sample are labeled. The dashed line gives the approximate boundary between thin and thick disk (metal poor) stars.

thick disk objects. Their classification is based on the galactic kinematics of these stars. Since R Vir is close to the colour limit and has a small LSR velocity, it could also be a thin disk star. Z Oph is a peculiar object and discussed below.

3.1. *Z Oph*

Despite its longer period we included the star Z Oph largely because of a remarkable figure presented by Keenan (1966) of Mira spectral type at maximum light as a function of period. In this figure Miras form a quite broad but nonetheless well defined distribution as a function of spectral type but Z Oph stands alone apparently having a period twice what would be indicated for its spectral type. Now, several decades after the Keenan paper, GCVS still lists no other Mira variable with a K spectral type at maximum and a period of more than 300 days. A key to understanding Z Oph may be a note in the Keenan article. Keenan comments that Z Oph represents a Mira with an extreme case of line weakening. Due to the extreme weakness of the absorption lines the spectral type could only be determined from the spectral shape (Keenan 1966).

We have compiled photometric data from the literature for a set of 20 Miras with periods between 340 and 360^{d}, i.e. close to Z Oph's value. Among these stars, Z Oph has the bluest near IR colours. Fitting two black bodies through the visual, near IR and IRAS photometry (Kerschbaum & Hron 1996) gives the highest stellar temperature among all the comparison objects. This confirms the very early spectral type. The high photospheric temperature and radial velocity can be best explained by a low metallicity. This is strongly supported by the selective line weakening very strongly expressed in this star (Keenan 1957). The infrared amplitude at 1μm is about $1\overset{m}{.}1$ (Lockwood & Wing 1971), which is a rather typical value. Z Oph has the bluest IRAS [12]–[25] colour among the 340–360^{d} Miras.

The center-of-mass velocity is a critical value for our investigation. For Miras, reliable data are provided mainly by radio measurements. None of the stars in our sample have detected thermal microwave lines which typically give the best information. Z Oph does not have SiO or OH masers detected (Benson & Little-Marenin 1996) nor are there any reports of thermal microwave lines. The velocity information is limited to a General Catalogue of Radial Velocities listing of -78 km s^{-1} and an analysis of optical spectra (Willson et al. 1982) giving a stellar velocity of -86 km s^{-1}. Willson et al. (1982) measured a velocity difference of 21 km s^{-1} in doubled atomic lines in the optical wavelength range and we adopt their value for the velocity of Z Oph.

An argument against metal-poor status for Z Oph can be made from galactic kinematics. While the spectral characteristics indicate a metal poor object, the galactic kinematics of Z Oph are compatible with a normal disk star (Alvarez et al. 1997). However the galactic coordinates of Z Oph and the small fraction of metal poor Miras make a kinematic assignment quite uncertain.

3.2. *RT Cyg*

The large negative radial velocity and short period of RT Cyg clearly mark this star as a metal poor object. From optical spectra Merrill (1952) finds a velocity difference between absorption and emission lines of approximately 10 to 12 km s^{-1}. Willson et al. (1982) found line doubling in optical atomic lines with a velocity difference of 15 km s^{-1}. As for Z Oph there is no microwave data and the Willson et al. value for the center-of-mass velocity is used for this investigation. Little et al. 1987 find Tc absent from the spectrum of RT Cyg.

3.3. *SS Oph*

This star combines a low space velocity with a period of only 180 days. The period strongly supports the classification of this object as an intermediate population Mira. Variability in period is noted by Vardya (1989). The radial velocity is poorly known. Neither OH (Sivagnanam et al. 1988) nor SiO maser emission (Deguchi et al. 1986) has been detected.

3.4. *R Cet*

R Cet is a well studied object. Both OH and SiO masers are known from this star. The OH maser gives an accurate stellar velocity of 41 km s^{-1} with a circumstellar expansion velocity of 4 km s^{-1} (Sivagnanam et al. 1989). Not enough infrared data have been collected to derive the radial velocity amplitude.

3.5. *X Mon*

There is little in the literature concerning X Mon. This star has been variously classified as a Mira or a semiregular variable (see Sect. 4). The GCVS reports significant variations in period length (145 to 169 d) and amplitude. For X Mon Wallerstein

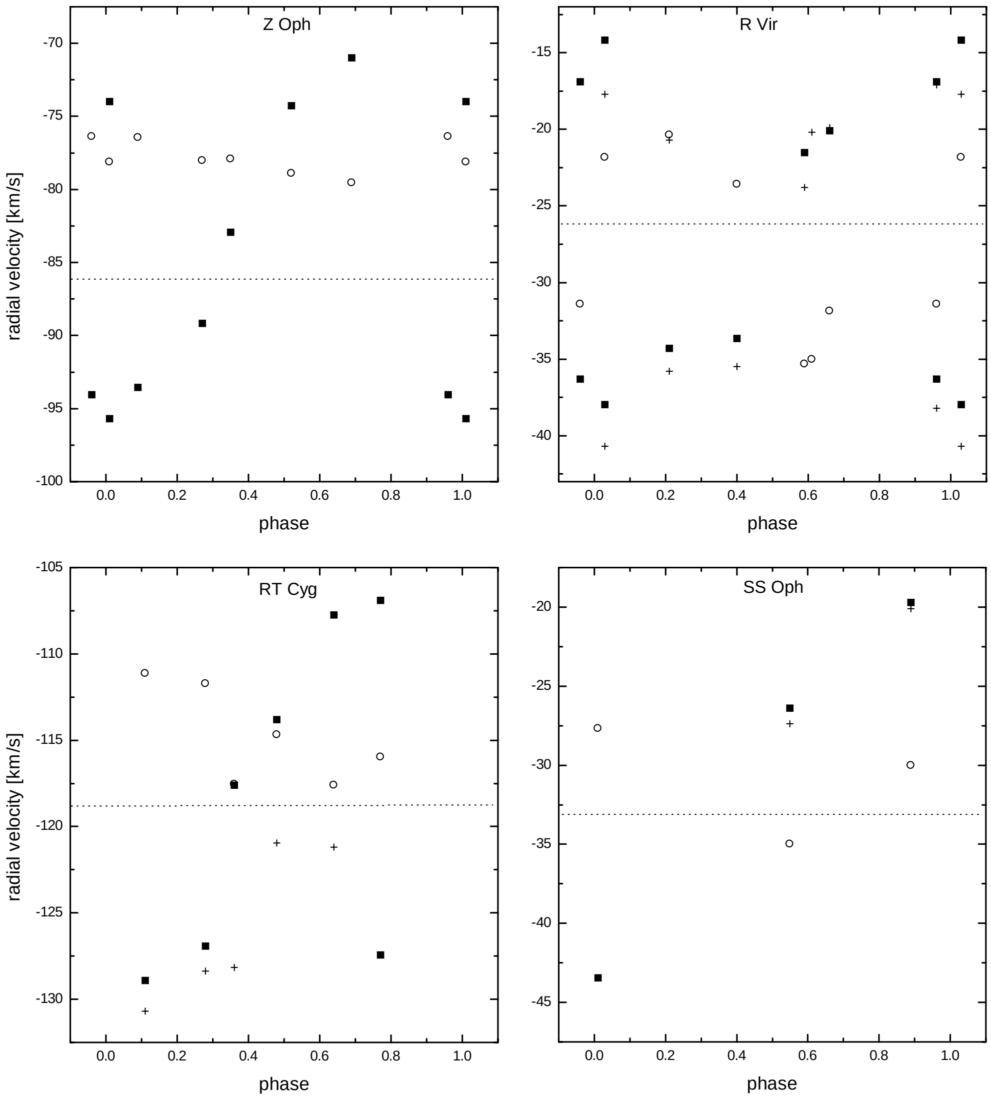

Fig. 2. Radial velocities of CO 2-0 and Ti lines versus phase. The filled boxes denote CO lines of high excitation, the open circles CO lines of low excitation and the crosses Ti lines. The velocities plotted here were determined by the measuring of line core positions.

& Dominy (1988) give a velocity derived from absorption lines of 161 to 164 km s^{-1} while hydrogen emission lines give 131 km s^{-1}. Not enough infrared data have been collected to derive the radial velocity amplitude.

3.6. R Vir

SiO maser emission (v=1, 1-0) was reported in the spectrum of R Vir by Dickinson et al. 1986) and by Jewell et al. (1991). Dickinson et al. note that the velocity spread of the SiO emission gives a lower bound to the velocity spread of OH emission (which was not detected in this star). Since the OH velocity spread is very small in short-period Miras (Dickinson et al. (1986), the SiO velocity of -29 km s^{-1}, must be within a few km s^{-1} of the stellar velocity. Radial velocities from the cross correlation of absorption features were measured from optical spectra by Barbier et al. (1988). These vary between -24 and -32 km s^{-1} heliocentric. Similar to SS Oph, R Vir has a rather low radial velocity for an old object.

R Vir has no Tc in its spectrum (Little et al. 1987). No 10 μm feature was found in the IRAS LRS spectra (Little-Marenin & Little 1990), but an infrared excess at 25 and 60 μm relative to the 12μm flux has been found by Stencel & Backman (1991). A low mass-loss rate of $0.6.10^{-7}$ $M_{\odot}$/yr was determined by Jura (1994).

4. Results

Radial velocities measured from the 2μm region spectra are plotted in Fig. 2 against phase. Most of the data were taken from only one or two adjacent cycles. An estimation of the phase was done using maxima and minima given by the AAVSO (Mattei 1981–87).

Line doubling of CO lines was present in some of the spectra around maximum light. A model of atmospheric dynamics of these stars derived from the velocity analysis is discussed in previous papers of this series. Line doubling might not have been found in some spectra due to line blends. Typically CO line doubling was detected only for those few CO lines in our spectral range where the high excitation CO line is not located close to a low CO excitation line. For Z Oph at phase 0.94, where one would expect to see line doubling, we could detect it only for the R84 line and this is therefore not shown in Fig. 2.

The amplitude of the radial velocity variations derived from the high excitation CO lines is about 20 to 25 km s^{-1} in all of our intermediate population Miras. The high excitation CO lines show a well defined S-shaped radial velocity curve in the four well sampled objects. There seems to be no significant shift between the maximum of the visual light curve and the minimum radial velocity. The low excitation CO lines typically show only very small variations in radial velocity (5 to 7 km s^{-1}). In RT Cyg and SS Oph these changes are more prominent than in Z Oph. The atomic titanium lines in the 2 micron region have the same velocity behavior as the high excitation CO lines.

For R Cet and X Mon (for each of them we have two spectra) a radial velocity amplitude could be estimated from comparison with other velocity curves. For R Cet the velocity curve appears similar to results from RT Cyg and must have an amplitude of 20 to 25 km s^{-1}. However, for X Mon we estimate an amplitude of only about 10 to 15 km s^{-1}. HSH found a similar amplitude for X Oph, a SRa variable. These stars have other similarities: They have the same visual amplitude and similar J-H and H-K colours. X Mon was originally classified a SRa. In a J-H versus H-K plot both stars are located at the border between Miras and SRas (Kerschbaum & Hron 1994). This is a tentative conclusion since velocities were not measured at enough phases of the X Mon light cycle to exclude an underestimation of the star's amplitude.

R Vir may behave slightly differently. The variations of the high excitation CO lines and the Ti lines seem to be a bit more complex with a bump in the rising part of the velocity. Line doubling is present at least at two phases. The Ti lines are very weak in the spectra of R Vir and were difficult to measure. The large radial velocity amplitude excludes misclassification of R Vir as a SR variable as suggested by the SiO data (Dickenson et al. 1986). Atypical strong variations (up to 15 km s^{-1}) were found in the low excitation CO lines in R Vir. Low excitation CO are formed over an extended atmospheric region (HHR). The very weak Ti lines suggest that R Vir is metal poor. A low metal abundance would alter the opacity, atmospheric structure, and mass-loss of this star. Insufficient data exist to show whether these features are a single event or observable in every cycle of R Vir. Not enough stars were monitored to derive if this behavior is observed in other Miras, too.

The excitation temperatures and isotopic ratios $^{12}C/^{13}C$ derived are listed in Table 2. Isotopic ratio on the order of 10 to 20 are typical for bright, thin disk Miras. The low isotopic ratio is consistent with the lack of photospheric Tc in these stars (see above; Little et al. 1987). The excitation temperatures derived for the intermediate population Miras fall within the range of values found in HHR, HSH and HLS for Miras with higher metallicity at similar phases.

Metal-poor and solar metallicity Miras share many basic characteristics. Both in metal poor and metal-rich Miras the low excitation CO lines show only small radial velocity variations and probably no periodic changes. The S-shaped variations of the infrared atomic lines and high excitation CO lines are also found in both types of Miras. This similarity suggests also a similar structure of the atmosphere of these variables and that also the indicators of the different atmospheric layers can be used in an analogous way. We note, that this similarity is not necessarily in contradiction with the differences found in the shapes of the visual light curves. Visual light variations are dominated by changes in TiO absorption which probably originates further out and is much more sensitive to temperature than the high excitation CO lines studied here.

Table 2. Isotopic ratios and excitation temperatures for intermediate population Miras.

GCVS name	phase/ date	$^{12}C/^{13}C$ uncertainty in ()	excitation temperature
X Mon	86 Mar 21	10 (+10 −4)	3000
R Vir	0.41	10 (+10 −2)	3000
Z Oph	0.52	10 (+10 −4)	3500:
R Cet	85 Sep 01	4 (+10 −1)	2750:

5. Discussion

5.1. Z Oph

The period and the radial velocity amplitude of the high excitation CO lines in Z Oph look exactly like that of any metal-rich Mira observed. On the other hand it is the only Mira listed in the GCVS with a spectral type in maximum earlier than M0 and a period of more than 300 days. To determine the evolutionary status of this object we assume that the star is metal poor ($Z/Z_\odot$= 0.3) with a mass between 0.6 and 0.8 solar masses and has an effective temperature of 3500K (from J-K and the star's mean spectral type). Then it is only slightly brighter than the calculated AGB-tip (Vassiliadis & Wood 1993). The calculation of the AGB brightness uses a typical mass loss. The difference between the observed and calculated positions on the HR diagram could be explained by the assumption that Z Oph has a very low mass-loss rate for its period, which would allow the star to stay longer on the AGB. The low mass-loss rate is evident from the IRAS colours of this star indicating no circumstellar shell.

5.2. The pulsation mode of long period variables

5.2.1. Previous work based on atmospheric kinematics

Compared with the results for metal-rich Miras (HHR, HSH, HLS) the radial velocity amplitude in the infrared of the high excitation CO lines is almost the same for the short-period Miras and Z Oph. Therefore we find that an amplitude of 20 to 30 km s^{-1} is typical for all Miras with no obvious dependency on period, metallicity or chemistry. On the other hand, for Semiregular Variables (SRVs) with periods comparable to the short-period Miras, Hinkle et al. (HLS) found a factor of two lower radial velocity amplitudes. Do these results mean that all Miras pulsate in the same mode and that the SRV's pulsate in a higher mode than the Miras? Do they mean that the Miras are fundamental mode pulsators? An interpretation of velocity variations in terms of pulsation modes in principle requires a detailed radiative transfer calculation based on dynamical model atmospheres (e.g. Bessell et al. 1996, Windsteig et al. 1997). Comparing our results for the Miras with the work of Bessell et al., the pulsation mode for all Miras would indeed be the fundamental. Given the large difference in the amplitudes between Miras and SRV's, the SRV's would then pulsate in the first (or higher) overtones.

Dynamical pulsation models (Bessell et al. 1996, Ya'ari & Tuchman 1996, Willson 1998) provide radius changes for different Lagrangian mass zones of the star. Assuming that the observed lines always come from the same mass zone (e.g. Tuchman 1991), the integrated radial velocity curve gives the observed radius change in meters of one mass element. Together with an assumed equilibrium radius, this change can be converted into fractions of the stellar radius and compared with the theoretical prediction. However, the observed line doubling and full radiative transfer calculations (Windsteig et al. in preparation) indicate that what we see is the movement of more than one photospheric layer. Furthermore, the direct integration of the full velocity curves (i.e. assuming that we see only one layer) typically corresponds to radius changes of a factor of two or more which is significantly larger than the results from interferometric measurements (e.g. van Belle et al. 1996). Similarly the slope of the velocity curve interpreted naively implies an unrealistically low surface gravity. The same discrepancy also arises from the rather large observed changes in the molecular excitation temperature of almost 2000 K (HLS) which would also correspond to a radius change of a factor of two in a dynamical model atmosphere.

In view of these facts and since the dynamical models are still in their beginnings we have looked for an alternative method to derive the radius changes.

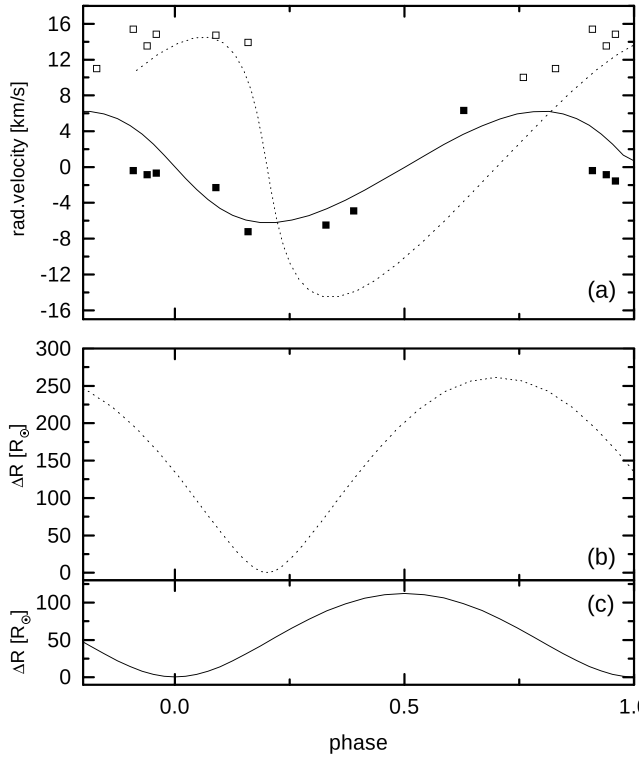

Fig. 3a–c. Approximation of two pulsating mass zones in R Aur. **a** Observed radial velocity variations and the derivatives of two cycloids shifted in phase by 0.2. Solid boxes were approximated by the solid line, open boxes by the dotted line. For better illustration some data points were repeated. **b**, **c** Corresponding variations in radius (cycloids) for the two zones. The phase shown corresponds to the cycloid with the smaller amplitude, visual phase is slightly shifted. Note that the plot does not represent the relative positions of the two zones in the stellar atmosphere.

5.2.2. A method for estimating the radius changes from the rv-curve

To estimate the radius variations of a single mass zone located near the classical stellar radius it is necessary to separate the different mass zones contributing to the total velocity variation of a given line.

Guided by the observed line doubling we approximate the velocity variations by the combination of two mass zones. The typical shapes for the movement of such mass zones (e.g. Figs. 1–3 of Bessell et al. 1996, Fig. 1 of Höfner & Dorfi 1997) were described by two phase shifted cycloids (e.g. Hazewinkel 1995) of different shape and amplitude corresponding to the two zones (Fig. 3, middle and lower panel). The derivative of the cycloid with the smaller amplitude (deeper zone in the atmosphere according to the models) was fitted to the lines showing outflow and high excitation temperature (phases between 0.0 and 0.25). The amplitude of the second cycloid (outer mass zone) was given by the part of the curve showing an inward motion and lower excitation temperatures (phases between 0.75 and 1.0) and by the condition to be symmetric in velocity around the stellar velocity. The velocity asymmetry in phase of the second cycloid and the phase shift between the cycloids was determined from the phase interval where line doubling was visible. However, the second cycloid will be used in this paper only to illustrate the method and will not be used in the discussion concerning the mode of pulsation.

The application of the method is illustrated in Fig. 3. The upper panel shows the fitting of the radial velocity variations for R Aur (HLS), in the middle and the lower panel the corresponding motion of the two mass zones approximated by cycloids is plotted. The radius change given is only relative to the deepest point reached by the mass shell. A further location of the shells within the stellar atmosphere is not possible except that the two trajectories will of course not cross each other. R Aur was selcted as it has a very well sampled and typical radial velocity curve and a well known center of mass velocity. Due to the phase shift (which is also seen in the dynamical models) and the different shape of the trajectory, line doubling occurs.

The cycloid closer to the stellar center is the one that will be compared with the results from model calculations.

It is clear that the use of only two shells is still a significant simplification but at least it allows for the observed line doubling. Contributions to the radial velocity curve come from several shells changing their shape and radius within the range of the two shells selected for the illustration. However, the fact that two clearly separated components are visible during line doubling indicates that the contributing layers can be roughly approximated by two shells.

A fit with the derivatives of cycloids is only possible for well sampled velocity curves. To be able to deal with the other cases we replaced the integration of cycloids by simple interpolations and piecewise integrations. Inspection of the radial velocity curves shows two interesting features common to all Miras observed up to now: The velocity change is almost linear between phases 0.2 and 0.8 and the center-of-mass velocity is reached close to phase 0.4. These facts allow a linear and therefore easy approximation of the inward movement observed. We decided to integrate half a period starting from the phase when the velocity of the CO lines is identical with the center of mass velocity. An integration of this inward movement can therefore be seen as an estimate of the radius variations of an outer layer. Inspection of Fig. 3 shows, however, that this approximation covers only a part of the whole radius changes of the outer shell. For defining the inner mass zone we directly integrated the velocities of the line components which show an outward motion, i.e. the other half of the light cycle. If the coverage of this part of the cycle is not well enough we could derive only a lower limit of the variations. These simpler integrations were also applied to the well sampled light curves and served as a check of the reliability compared to the cycloid approach.

5.2.3. Deriving absolute radius variations

For the comparison with the pulsation models we also need the absolute radius variations. The excitation temperatures near maximum light indicate that the minimum radius and hence also the inner mass zone should be located quite deep in the photosphere. Therefore we calculated stellar radii ($R_\star$) from the asymptotic giant branch models of Bessell et al. (1989). The luminosities were calculated from the P/L relation for Miras in Alvarez et al. (1997). We also computed radii for metal poor ($1/16 Z_\odot$) stars. Based on these results and to account for the uncertainty in mass, luminosity, temperature and metallicity we have adopted a range of values for $R_\star$ for each object. These radii were then used as the minimum radius of the mass zone.

Low metallicity would have a significant impact on the calculated size of a 350^d period Mira. As this might be relevant for Z Oph, three radii were derived to span also the range of low metallicity. The radii are listed in Table 3 together with the ratio of maximum to minimum radius obtained from the above mentioned approaches. X Mon and R Cet where included, too, although the two datapoints available for each of these two stars do not allow a very good approximation. For SS Oph the cycloid approach could not be used due to the bad phase coverage of the radial velocity curve. For comparison with long-period Miras R Aur was included, too. The radial velocity data for this star have been published by Hinkle, Lebzelter & Scharlach (1997).

Table 3. Stellar parameters and radius changes for the Miras of our sample. R Aur is included for comparison. Column 2 lists the period used for calculation of the stellar radii given in column 3. Columns 4, 5 and 6 list the ratio of maximum to minimum radius from integration of different parts of the radial velocity curve and from the cycloid approximation (see text), respectively.

Star	Period [d]	$R_\star$ [$R_\odot$]	R_{max}/R_{min} rv-curve (0.4–0.9)	rv-curve (0.9–0.4)	cycloid
R Aur	450	400	1.64	1.31	1.38
		500	1.31	1.25	1.29
Z Oph	350	200	2.10	1.45	1.64
		300	1.73	1.30	1.43
		400	1.55	1.23	1.32
RT Cyg	150	100	2.12	1.36	1.57
		200	1.56	1.18	1.29
SS Oph	150	100	1.76	–	–
		200	1.38	–	–
R Cet	150	100	–	>1.35	–
		200	–	>1.18	–
X Mon	150	100	1.54:	–	–
		200	1.27:	–	–
R Vir	150	100	1.55	>1.39	1.50
		200	1.28	>1.20	1.25

All presented methods depend strongly on the accuracy of the center-of-mass velocity as it defines the border between inward and outward moving material. Problems in fitting the two cycloids can be explained by a wrong center-of-mass velocity. While in principle the stellar velocity is always reached shortly before the visual light minimum, more radial velocity curves would be needed to use this fact for a reliable estimate of the stellar velocity. Changing the center-of-mass velocity by a few km s^{-1} can lead to changes in R_{max}/R_{min} of about 10 percent. For RT Cyg we adopted a stellar velocity of -124 km s^{-1}, differing from the published results (see Table 1). This produced a better fit with the two cycloids model and the typical radial velocity curves. The same would also apply to Z Oph, but as changes are not that significant we used the velocity given in the literature.

5.2.4. Interpretation of the results

Before interpreting the results in Table 3 one should remember that the cycloid approximation (column 6) should give the best estimate of the radius change of a mass zone located deep in the atmosphere. The integration of the outward moving part (column 5) should give slightly smaller radius changes in view of the slightly incomplete coverage of the total radius change. This is also seen in the table. The integration of the inward moving part (column 4) covers only around half of the total movement for an outer zone. Since this zone will in general show larger radius variations we expect the computed radius variations to be generally larger than in the other two cases and that is actually the case. Thus the values listed in the table are quite consistent with each other.

It can be seen that the typical radius variation is between 20 % and 70 %. We note that adopting $R_\star$ as the *mean* radius of the inner mass zone changes the above ratios only by a few percent.

Our estimates of the radius changes can now be compared with the predictions of pulsation models and dynamical model atmospheres. Bessell et al. (1996) find a ratio of 1.4 for fundamental mode pulsation and 1.05 for first overtone. Willson (1998) gives 1.21 for fundamental mode and 1.04 for first overtone. Even though our approach uses some simplifications, these numbers make overtone pulsation quite unlikely for all the Miras in our sample and also the longer period stars represented here by R Aur. The results on X Mon and R Cet are based on only two datapoints and are therefore rather uncertain. We note that Ya'ari & Tuchman (1996) find fundamental mode values between 1.7 and 2.4 from their long-term non-linear simulations. However their models are very cool and therefore it is not clear to which degree they are representative for typical galactic Miras.

Van Belle et al. (1996) derived radii and radius variations from interferometry in the K band for 18 Miras. A part of their sample has been monitored for radial velocity variations of CO Δv = 3 lines by HSH (1989). For two of these objects van Belle et al. measured a maximum and a minimum radius. For X Oph they derive a difference between the maximum and the minimum radius of 68 $R_\odot$ with a minimum radius of 350 $R_\odot$. Integration of the inward moving part of the radial velocity curve (phases 0.4 to 0.9) leads to a variation of 119 $R_\odot$. The outward moving part gives a variation of 76 $R_\odot$. Using a stellar radius of 400 $R_\odot$, according to a period of 331^d, the ratio $R_{\rm max}/R_{\rm min}$ is therefore between 1.3 and 1.19. The variations of the inner shell are very similar to the results by van Belle et al. of 1.19. A similar agreement is found for R Aql, where they find a radius variation of 97 $R_\odot$ compared to our results giving 112 $R_\odot$ from the inward moving part. Due to bad phase coverage of the radial velocity curve of R Aql the outward moving part could not be used.

X Oph is one of the stars with a significantly smaller radial velocity amplitude. The small ratio $R_{\rm max}/R_{\rm min}$ might suggest that the small radial velocity amplitude is connected to a different pulsation mode.

6. Conclusions

The research presented in this paper allows the following conclusions:

1. The amplitude of the radial velocity variations for Mira variables is nearly independent of period for periods between 150 and 400 days.
2. The amplitude does not depend on metallicity.
3. It seems very likely that all Miras pulsate in the same mode.
4. The comparison of our results with dynamic model atmospheres strongly suggests that Miras are fundamental mode pulsators.

Although the short-period Miras form only a small group of objects they can provide important information on the effect of smaller periods and lower metallicity on the pulsational properties of Miras and on the mechanisms of mass loss. This would be an important input for theoretical models (e.g. Feuchtinger et al. 1993). Models like the ones by Windsteig et al. (1997) now allow the calculation of synthetic single line profiles in a dynamical atmosphere. We plan to use these models for better understanding the origin of the components contributing to the infrared spectra in both Miras and semiregular variables.

The current observed sample of objects is small. Infrared spectroscopy and photometry for a larger sample would allow statistical analysis.

Acknowledgements. This work was supported by the *Fonds zur Förderung der wissenschaftlichen Forschung* under project number S07308-AST, by the *Austrian Ministery for Science and Arts ("kurzfristige wissenschaftliche Arbeiten im Ausland")*, and by the *Österreichische Forschungsgemeinschaft*. This research has made use of the Simbad database operated at CDS, Strasbourg, France. We thank D. Stultz for assistance at the telescope. We gratefully acknowledge the support of the NOAO director, Dr. Sidney Wolff, in making the KPNO 4 meter telescope available to us for daytime observing. Discussions with Drs. Thomas Barnes, Nicholas Suntzeff, and Robert Wing contributed to the research on Z Oph. We thank Ms.Diana Johnson and Mr.Werner Scharlach for assistance with the data reduction. We wish to thank Dr. Alfred Gautschy and Dr. Michael Feuchtinger for enlightening discussion.

References

Alvarez R., Mennessier M.-O., 1997, A&A 317, 761
Alvarez R., Mennessier M.-O., Barthès D., Luri X., Mattei J.A., 1997, A&A 327, 656
Barbier M., Petit H., Mayor M., Mennessier M.O., 1988, A&AS 72, 463
Barnbaum C., Hinkle K.H., 1995, AJ 110, 805
Benson P.J., Little-Marenin I.R., 1996, ApJS 106, 579
Bessell M.S., Brett J.M., Scholz M., Wood P.R., 1989, A&AS 77, 1
Bessell M.S., Scholz M., Wood P.R., 1996, A&A 307, 481
Deguchi S., Claussen M.J., Goldsmith P.F., 1986, ApJ 303, 810
Dickinson D.F., et al., 1986, AJ 92, 627
Feast M., 1963, MNRAS 125, 367
Feuchtinger M.U., Dorfi E.A., Höfner S., 1993, A&A 273, 513
Hall D.N.B., Ridgway S.T., Bell E.A., Yarborough J.M., 1979, Proc. SPIE 172, 121
Hazewinkel M.(ed.), 1995, In: Encyclopaedia of Mathematics. Kluwer, Dordrecht
Hashimoto O., 1994, A&AS 107, 445
Hinkle K.H., 1978, ApJ 220, 210
Hinkle K.H, Hall D.B., Ridgway S.T., 1982, ApJ 252, 697 (HHR)
Hinkle K.H., Lebzelter T., Scharlach W.W.G., 1997, AJ 114, 2686 (HLS)
Hinkle K.H., Scharlach W.W.G., Hall D.N.B., 1984, ApJS 56, 1 (HSH)
Hoffleit D., 1964, Catalogue of Bright Stars. 3rd edition, New Haven, Connecticut

Höfner S., Dorfi E.A., 1997, A&A 319, 648
Hron J., 1991, A&A 252, 583
Hron J., 1998, in preparation
Hron J., 1993, In: Weinberger R., Acker A. (eds.) Planetary Nebulae. Proc. IAU Symp. 155, Kluwer, Dordrecht, 327
Jewell P.R., et al., 1991, A&A 242, 211
Jura M., 1994, ApJ 422, 102
Jura M., Kleinmann S.G., 1992, ApJS 79, 105
Keenan P.C., 1957, AJ 62, 244
Keenan P.C., 1966, ApJS 13, 333
Keenan P.C., Garrison R.F., Deutsch A.J., 1974, ApJS 28, 271
Kerschbaum F., Hron J., 1994, A&AS 106, 397
Kerschbaum F., Hron J., 1996, A&A 308, 489
Kholopov P.N., et al., 1985-88, General Catalogue of Variable Stars. 4th edition, Moscow (GCVS)
Little S.J., Little-Marenin I.R., Hagen-Bauer W., 1987, AJ 94, 981
Little-Marenin I.R., Little S.J., 1990, AJ 99, 1173
Lockwood G.W., Wing R.F., 1971, ApJ 169, 63
Mattei J.A., 1981-87, AAVSO Bulletin 44-50
Menzies J.W., Whitelock P.A., 1985, MNRAS 212, 783
Merrill P.W., 1952, ApJ 116, 523
Norton R.H., Beer R., 1976, J.Opt.Soc.Am. 66, 259
Robertson B.S.C., Feast M.W., 1981, MNRAS 196, 111
Sivagnanam P., Le Squeren A.M., Foy F., 1988, A&A 206, 285
Sivagnanam P., Le Squeren A.M., Foy F., Tran Minh F., 1988, A&A 211, 341
Stencel R.E., Backman D.E., 1991, ApJS 75, 905
Tuchman Y., 1991, ApJ 383, 779
van Belle G.T., Dyck H.M., Benson J.A., Lacasse M.G., 1996, AJ 112, 2147
Vardya M.S., 1988, A&AS 73, 181
Vardya M.S., 1989, A&A 209, 165
Vassiliadis E., Wood P.R., 1993, ApJ 413, 641
Wallerstein G., Dominy J.F., 1988, ApJ 326, 292
Willson L.A., 1998, Proc. Variable Stars: New Frontiers, PASPC, in press
Willson L.A., Wallerstein G., Pilachowski C.A., 1982, MNRAS 198, 483
Wilson E.R., 1963, General Catalogue of Stellar Radial Velocities. Washington D.C.
Wilson R.E, Merrill P.W., 1942, ApJ 95, 248
Windsteig W., Loidl R., Höfner S., Dorfi E.A., 1997, In: Bedding T.R. (ed.) Fundamental Stellar Properties: the Interaction between Observations and Theory. Poster Proc. IAU Symp. 189, School of Physics, Univ. of Sidney, 172
Wyatt S.P., Cahn J.H., 1983, ApJ 275, 225
Ya'ari A., Tuchman Y., 1996, ApJ 456, 350